[15] Gini, F. (1997)
A cumulant-based adaptive technique for coherent radar detection in a mixture of K-distributed clutter and Gaussian disturbance.
IEEE Transactions on Signal Processing, **45** (June 1997), 1507–1519.

[16] Gini, F., Greco, M. V., Farina, A., and Lombardo, P. (1998)
Optimum and mismatched detection against K-distributed plus Gaussian clutter.
IEEE Transactions on Aerospace and Electronic Systems, **34** (July 1998), 860–876.

[17] Kelly, E. J. (1986)
An adaptive detection algorithm.
IEEE Transactions on Aerospace and Electronic Systems, **23** (Nov. 1986), 115–127.

[18] Khatri, C. G., and Radhakrishna Rao, C. (1987)
Effects of estimated noise covariance matrix in optimal signal detection.
IEEE Transactions on Signal Processing, **35** (May 1987), 671–679.

[19] Korado, V. A. (1968)
Optimum detection of signals with random parameters against the background of noise of unknown intensity under conditions of costant false alarm probability.
Radio Engineering and Electronic Physics, **13** (1968), 969–972.

[20] Picinbono, B., and Vezzosi, G. (1970)
Detection d'un signal certain dans un bruit non stationnaire et non Gaussien.
Annales des Telecomm., **25** (1970), 433–439.

[21] Rangaswamy, M., and Michels, J. H. (1997)
A parametric multichannel detection for correlated non-Gaussian random processes.
In *Proceedings of 1997 National Radar Conference*, Syracuse, NY, May 1997, 349–354.

[22] Reed, I. S., Mallet, J. D., and Brennan, L. E. (1974)
Rapid covergence rate in adaptive arrays.
IEEE Transactions on Aerospace and Electronic Systems, **AES-10** (Nov. 1974), 863–885.

[23] Richmond, C. D. (1996)
Adaptive array signal processing and performance analysis in non-Gaussian environments.
Ph.D. dissertation, Massachusetts Institute of Technology, Cambridge, MA, May 1996.

[24] Richmond, C. D. (1996)
A note on non-Gaussian adaptive array detection and signal parameter estimation.
IEEE Signal Processing Letters, **3** (Aug. 1996), 251–252.

[25] Robey, F. C., Fuhrmann, D. R., Kelly, E. J., and Nitzberg, R. (1992)
A CFAR adaptive matched filter detector.
IEEE Transactions on Aerospace and Electronic Systems, **28** (Jan. 1992), 208–216.

[26] Sangston, K. J., and Gerlach, K. R. (1994)
Coherent detection of radar targets in a non-Gaussian background.
IEEE Transactions on Aerospace and Electronic Systems, **30** (Apr. 1994), 330–340.

[27] Sangston, K. J., Gini, F., Greco, M. V., and Farina, A. (1999)
Structures for radar detection in compound-Gaussian clutter.
IEEE Transactions on Aerospace and Electronic Systems, **35**, 1 (Apr. 1999), 445–458.

[28] Scharf, L., and Lytle, D. W. (1971)
Signal detection in Gaussian noise of unknown level: An invariance application.
IEEE Transactions on Information. Theory, **IT-17** (July 1971), 404–411.

[29] Ward, K. D., Baker, C. J., and Watts, S. (1990)
Maritime surveillance radar. Part 1: Radar scattering from the ocean surface.
IEEE Proceedings, Pt. F, **137** (Apr. 1990), 51–62.

An Analysis of the Shadow Feature Technique in Radar Detection

Good target detection can be achieved by using shadow feature algorithms, particularly in heavy clutter environments. The performance enhancement of a shadow feature algorithm applied to a maximum likelihood constant false-alarm rate (ML-CFAR) detector is analyzed. Results show that detection performance is significantly improved.

I. INTRODUCTION

The concept of making use of the target shadow feature for detection has been discussed in [1–3]. As shown in Fig. 1, the shadow feature results when a portion of the ground is obscured by the target as seen from the radar; there will be no clutter returns for a number of range bins behind the target. Thus, by detecting these abrupt changes in clutter returns, a more reliable detection of the target can be obtained.

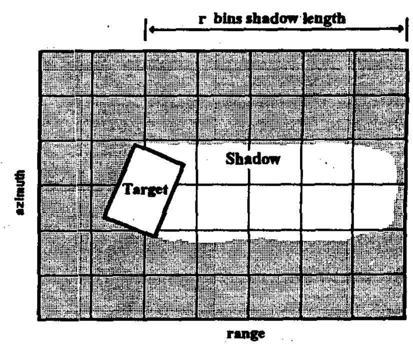

Fig. 1. Shadow effect.

Section II contains an analysis of the shadow feature technique, together with the method of implementation. Section III describes the results of the implementation. Section IV is the conclusion.

II. ANALYSIS OF SHADOW FEATURE ALGORITHM

The performance analysis of this algorithm is based on the conditional probability concept and on

Manuscript received June 23, 1993; revised April 12, 1995.

IEEE Log No. T-AES/35/3/06423.

0018-9251/99/$10.00

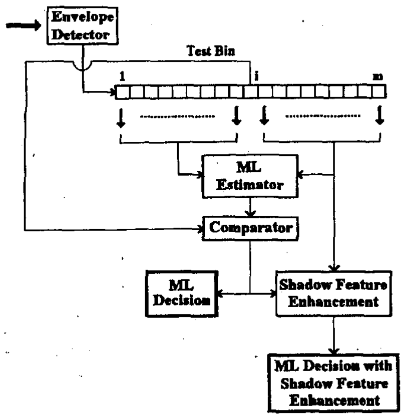

Fig. 2. ML-CFAR processor with shadow feature enhancement.

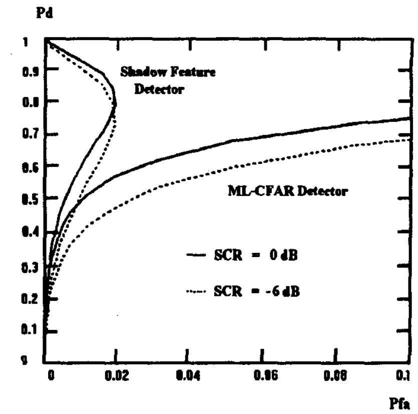

Fig. 3(a). Detection performance for $m = 5$, $r = 2$.

the assumption that there is only one target in the detection domain. Fig. 2 shows the block diagram of the detector processor [3]. We examine the hypothesis of a target in the test bin, i.e., the ith bin, as shown in the block diagram; see Fig. 2.

Let $P^i_{dt}(x)$ be the probability of successful target detection in the ith bin using a threshold value of x, and $P^i_{fa}(x)$ be the corresponding probability of false alarm. $P^i_{d,c}(x)$ is the probability of detection when the bin constitutes clutter-only signal returns, and $P^i_{d,s}(x)$ is the probability of shadow detection when the bin constitutes neither target nor clutter returns.

The shadow length can be estimated from the elevation/azimuth angles of the radar, the ground profile, and the expected target height. For a shadow length of r bins, the overall probability of a target detection $P_d(x)$ is equal to the probability of successful target detection in the test bin and shadow detection in the subsequent r bins:

$$P_d(x) = P^i_{d,t}(x) * \prod_{n=i+1}^{i+r} P^n_{d,s}(x). \qquad (1)$$

The overall probability of false alarm, $P_{fa}(x)$, is equal to the probability of false alarm in the test bin plus the probability of not detecting clutter signals for the subsequent bins:

$$P_{fa}(x) = P^i_{fa}(x) * \prod_{n=i+1}^{i+r} (1 - P^n_{d,c}(x)). \qquad (2)$$

By using (1) and (2), the performance of the shadow feature algorithm in terms of the P_d and P_{fa} can be obtained as a function of $P_{d,c}$, $P_{d,s}$, and the threshold value x. $P_{d,c}$ can be expressed as a function of the clutter characteristics in terms of the clutter cross section statistical distribution curve [5]. $P_{d,s}$ can be expressed as a function of the noise characteristics.

For the maximum likelihood constant false-alarm rate (ML-CFAR) detector and a Rayleigh target model in a Weibull clutter [3], the performance enhancement may be determined as follows. The probability of false alarm in the ith bin, $P^i_{fa}(x)$ is

$$P^i_{fa}(x) = \left(1 + \frac{x^2}{m}\right)^{-m}$$

and the probability of detection in a target-constituted bin $P^i_{d,t}(x)$ is

$$P^i_{d,t}(x) = \left(1 + \frac{x^2}{m(1 + \mathrm{SCR})}\right)^{-m}$$

where m is the number of bins considered in the ML-CFAR detector, and SCR is the signal-to-clutter voltage ratio. The probability of detection in a clutter-only bin $P^i_{d,c}(x)$ is

$$P^i_{d,c}(x) = \left(1 + \frac{x^2}{m}\right)^{-m}.$$

For the shadow bins, in which only noise exists, the probability of shadow detection $P^i_{d,s}(x)$ is

$$P^i_{d,s}(x) = 1 - (\text{Probability of Noise Detection}).$$

III. RESULTS AND DISCUSSIONS

Results for the shadow feature algorithm enhancement are calculated at different SCR levels. It is assumed that the signal and clutter are much larger than the noise amplitude. Figs. 3(a) and 3(b) compare the performance of the ML-CFAR detector with the shadow feature enhancement. The shadow feature algorithm provides better detection capability than the ML-CFAR only, limiting the P_{fa} to relatively low values. It can be considered that in the detector processor the original threshold of the ML-CFAR only is lower in order to improve the overall P_d with a corresponding increase in P_{fa}. However, the shadow feature algorithm compensates for this increase in P_{fa}, resulting in a better overall detection capability. Figs. 3(a) and 3(b) also reveal this, i.e., the shadow feature algorithm will have P_{fa} no greater than 0.02.

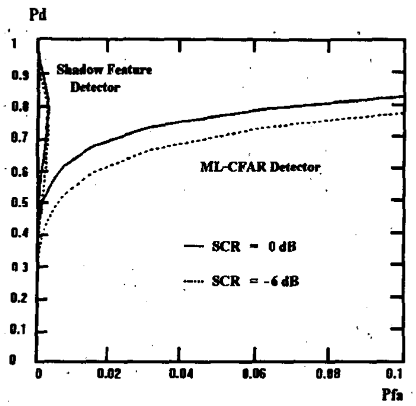

Fig. 3(b). Detection performance for $m = 7$, $r = 3$.

For small P_{fa}, such as 10^{-5} to 10^{-6}, the overall P_d for the shadow feature algorithm still exceeds that for the ML detector only, even for small estimated shadow length. However, this improvement diminishes as the false-alarm rate tends to zero.

IV. CONCLUSION

A performance analysis of the shadow feature algorithm is described in this letter together with detailed analytical results. These show that the algorithm is readily applicable to radar systems and is effective even in low signal-to-clutter environments below 0 dB.

S. W. LEUNG
JAMES W. MINETT
C. F. CHUNG
Electronic Engineering Dept.
City University of Hong Kong
83 Tat Chee Avenue
Kowloon, Hong Kong

REFERENCES

[1] Leung, S. W., Yeung, K. H., Tse, P. W., and Chow, W. S. (1990)
A target identification and recognition DSP algorithm for ground transport detection.
In *Proceedings of the Systems International Conference on Signal Processing '90 Beijing*, Beijing, 1990, 671–674.

[2] Leung, S. W., and Yeung, K. H. (1990)
Shadow feature enhancement in radar detection.
In *Proceedings of the 1990 International Symposium on Information Theory and Its Applications*, **1**, Hawaii (1990), 275–278.

[3] Leung, S. W., and Wong, C. H. (1991)
A shadow feature signal processing algorithm for radar systems.
In *Proceedings of the 1991 International Conference on Circuits and Systems*, China, June 1991, 452–455.

[4] Ravid, R., and Levanon, N. (1992)
Maximum-likelihood CFAR for Weibull background.
IEE Proceedings, Pt. F, **139**, 3 (June 1992).

[5] Skolnik, M. (1990)
Radar Handbook (2nd ed.).
New York: Hill, 1990, 2.16–2.26.

Effectiveness Boundaries of Interferometric SAR

Interferometric synthetic aperture radar (InSAR) ability to determine pixel elevation with a resolution derived from the interferometer phase resolution, is maintained as long as the interferometer phase change over the pixel does not exceed the phase resolution. This work investigates the surface coverage where this condition is met, determines the elevation resolution, and derives the ratio between elevation resolution and across-track resolution.

I. INTRODUCTION

In synthetic aperture radar (SAR) processing [1] the imaged pixel is located at one of the two intersections between three surfaces (Fig. 1): the range sphere,

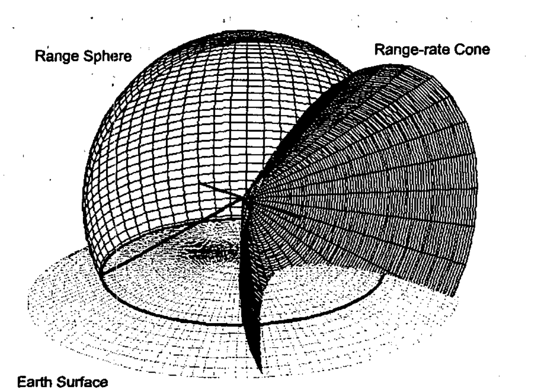

Fig. 1. Geometry of SAR processing.

the range-rate (Doppler) cone, and the Earth surface. The range sphere is centered at the antenna, which is also where the apex of the cone is located. The cone axis of symmetry is the velocity vector. The required knowledge of the Earth surface elevation makes this a two-dimensional (2-D) type of radar. In other words, if the surface elevation is known, the range and Doppler (range-rate) measurements can define the horizontal pixel location. An error in the assumed surface elevation will cause an across-track error in the pixel location. The pixel size is determined by the range and Doppler resolutions and by the geometry.

Manuscript received January 25, 1998; revised November 17, 1998 and March 17, 1999.

IEEE Log No. T-AES/35/3/06425.